H-7-01 (Invited) Extended Abstracts of the 2019 International Conference on Solid State Devices and Materials, Nagoya, 2019, pp399-400

Memory functions of magnetic skyrmion

Wataru Koshibae

RIKEN Center for Emergent Matter Science (CEMS), Wako, Saitama 351-0198, Japan

Abstract

Magnetic skyrmion, a swirling magnetic texture, has attracted much attention not only in the fundamental physics viewpoint but also in applications especially to memory function. Here, I will review the recent developments of studies on the skyrmion dynamics and discuss the potential applications to the skyrmion memory devices.

1. Introduction

Magnetic skyrmion is a topological magnetic texture characterized by the mapping from the two dimensional real space to the unit sphere, i.e., spatially distributed normalized magnetic moments $\mathbf{n}_\mathbf{r}$ represents the mapping from the two-dimensional spatial coordinate $\mathbf{r}$ to the vector $\mathbf{n}$ wrapping the unit sphere. Figure 1 shows the schematic figure of the magnetic skyrmion in two dimensions. In Fig.1 (a), the vortex like structure is in the ferromagnetic background and the winding plane of the magnetic moments is perpendicular to the radial direction of the circular magnetic texture. This is the Bloch skyrmion and is often observed in the chiral magnets. In Fig.1 (b), on the other hand, the winding plane includes the radial direction. This is called Néel skyrmion and is often found in the artificially composed super-lattice magnet. The Bloch and the Néel skyrmions are in the same topological class: Specifically, the wrapping number of the unit sphere by the magnetic moments

$$N_{sk} = \frac{1}{4\pi}\int d^2r\, \mathbf{n}_\mathbf{r} \cdot \left(\frac{\partial \mathbf{n}_\mathbf{r}}{\partial x} \times \frac{\partial \mathbf{n}_\mathbf{r}}{\partial y} \right), \qquad (1)$$

defines the topological index called the skyrmion number. This naturally has a sign and represents the vorticity of the swirling magnetic texture. For the Bloch and the Néel skyrmions, $N_{sk} = -1$ where z-axis is taken to be parallel to the external magnetic field and the core magnetic moment of the skyrmion is antiparallel to the magnetic field.

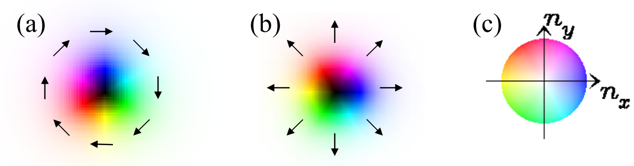

Fig. 1 Magnetic skyrmions. (a) Magnetic texture of the Bloch skyrmion. The arrows indicate the winding texture of the in-plane magnetic moments. (b) The same as (a), but for the Néel skyrmion. To represent the magnetic texture, the color code (c) is used.

In the earlier stage of the skyrmion study, the importance of the skyrmion from the application viewpoint was already discussed [1,2], i.e., the utilization of the skyrmion for the information carrier. It has been considered that the topological nature of the skyrmion assures a stable/robust memory function and also brings about an advantage for the manipulation/control by external forces. We theoretically study the creation, annihilation and current-driven motion of skyrmion by numerically solving Landau-Lifshitz-Gilbert equation. By the numerical study, we explore the optimal condition to control the skyrmion in the ferromagnetic background.

2. Skyrmion creation/annihilation

To utilize the skyrmion for the digital memory bit, the control technique for creation (write) and annihilation (erase) must be established. To create/annihilate the skyrmion in the ferromagnetic background, a topological transition is required: The topological stability of a skyrmion is often explained by the topological difference between the skyrmion and the perfect ferromagnetic state (F state). The difference is actually characterized by the skyrmion number, i.e., $N_{sk} = -1$ for the skyrmion but $N_{sk} = 0$ for the F state. Because of the difference in topology, the skyrmion cannot be reached from the F state within the continuous deformation of the magnetic texture. As a result, the skyrmion carries a (meta-) stability and is protected by a substantial magnitude of potential barrier. To overcome this barrier, a large energy enough to destroy the magnetic ordering is needed. We find that the spatial discontinuity of the shape of the system can reduce the potential barrier and useful to change the topology of the magnetic texture. On this strategy, we theoretically design the skyrmion memory devices controlled by electric field, magnetic field, local heating and other external stimuli [2].

3. Current driven skyrmion dynamics

The topology of the skyrmion is of crucial importance for the current-driven motion: Because of the vorticity of the swirling magnetic texture, a Magnus effect occurs along with the motion of the skyrmion. In particular, the velocity perpendicular to the force due to the impurity is induced by the Magnus effect, which results in avoiding the impurity during the skyrmion motion.

Besed on this unique feature, we theoretically develop new methods to drive the skyrmion [2,3]. Figure 2 shows an example. In this device structure, two layered skyrmion magnets are coupled antiferromagnetically. By applying the currents which are opposite to each other between the layers, the coupled skyrmion moves perpendicular to the current direction. We find that the velocity of the skyrmion in this device is enhanced by a factor $1/\alpha$ (α: Gilbert damping constant).

This is a strategy to develop high-speed skyrmion-manipulation method.

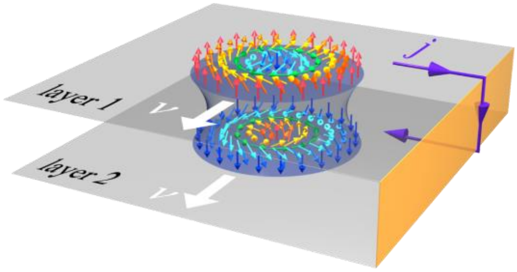

Fig. 2 A method to drive skyrmions [3]. The upper layer (layer 1) skyrmion antiferromagnetically couples with that in the lower layer (layer 2). The coupled skyrmions move perpendicular to the current *j*.

4. Skyrmion dynamics and disorder

The earlier experimental works have shown that the threshold current density to move the skyrmions in bulk-form chiral magnets is ~10^6A/m^2 being orders of magnitude smaller than that for magnetic domain wall motion. This was assumed to be an advantageous for technological application. However, it has been reported that the microscale-fabricated samples show very large threshold current density, e.g., the room-temperature skyrmion-devices by artificial thin-film heterostructures often show the threshold current density being 4 or 5 orders of magnitude larger than that of conventional bulk skyrmion magnets. In those samples, the stochastic skyrmion annihilation has also been observed.

We theoretically examine the current driven skyrmion dynamics in the system with disorder [4]. The skyrmion in the thin film form samples, the swirling magnetic texture forms a string through from top to bottom when the magnetic field is perpendicular to the film. Therefore, the skyrmion has the degrees of freedom along the magnetic field. In the system with disorder, the skyrmion motion brings the meandering dynamics to avoid the impurities (see Fig.3(a)). These degrees of freedom are missing for the shorter skyrmion, so that the impurity effect is enhanced. This appears as the large depinning threshold current and/or the stochastic skyrmion annihilation. For the longer skyrmion, on the other hand, we find an instability of the skyrmion string: During the skyrmion string motion, a rupture of the string occurs and at the broken point, a magnetic monopole-antimonopole pair is created (see Fig.3(b)). The monopole and antimonopole run along the skyrmion string, and finally, the skyrmion string totally disappears when it is a metastable structure. The skyrmion string is made from a large number of magnetic moments. On the skyrmion dynamics, the collision with impurities causes magnetic excitation on the skyrmion string. We find that the propagation and resonance of the collective magnetic excitation play crucial roles for the monopole-antimonopole pair creation and the skyrmion annihilation. This indicates that there is the optimal range of thickness for the topological stability of skyrmion. This result provides a way to design the skyrmion devices.

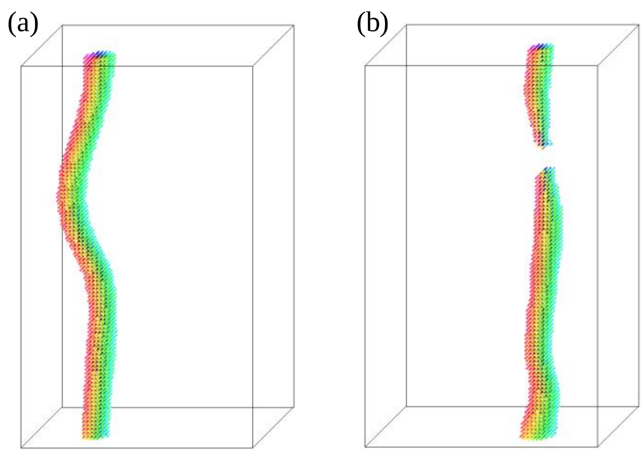

Fig. 3 Skyrmion string [4]. (a) An example of meandering skyrmion string structure. (b) An example of skyrmion string with monopole-antimonopole pair. To represent the magnetic textures, the color code Fig.1(c) is used.

Acknowledgements

This work was done in collaboration with Y. Kaneko, J. Iwasaki, M. Kawasaki, Y. Tokura and N. Nagaosa. We thank M. Ishida for technical assistance. This work was supported by JST CREST Grant Number JPMJCR1874, Japan, and JSPS KAKENHI Grant numbers 18H03676 and 26103006.

References

[1] As a review: N. Nagaosa, and Y. Tokura, Nat. Nanotechnol. **8** (2013) 899.
[2] W. Koshibae, Y. Kaneko, J. Iwasaki, M. Kawasaki, Y. Tokura and N. Nagaosa, Jpn. J. Appl. Phys. **54** (2015) 053001.
[3] W. Koshibae, and N. Nagaosa, Sci. Rep. **7** (2017) 42645.
[4] W. Koshibae, and N. Nagaosa, Sci. Rep. **9** (2019) 5111.